



Contents lists available at ScienceDirect

# Journal of Quantitative Spectroscopy & Radiative Transfer

journal homepage: [www.elsevier.com/locate/jqsrt](http://www.elsevier.com/locate/jqsrt)

## Simulation of light scattering by multilayer cross-gratings with the coupled dipole method

Patrick C. Chaumet\*, A. Sentenac

Institut Fresnel (Unité Mixte de Recherche 6133), Université d'Aix-Marseille III, Av. Escadrille Normandie-Niemen, F-13397 Marseille cedex 20, France

### ARTICLE INFO

#### Article history:

Received 17 October 2008

Received in revised form

17 December 2008

Accepted 18 December 2008

#### Keywords:

Coupled dipole method

Multilayer system

Periodic structure

### ABSTRACT

We adapt the coupled dipole method (CDM) to simulate light scattering by arbitrary dielectric structures that are periodic along two directions and embedded in a multilayer system. We calculate the near-field existing above isotropic gratings and provide comparisons with the classical Fourier modal method. We show that the CDM can deal easily with multilayer cross-gratings made of anisotropic material.

© 2009 Elsevier Ltd. All rights reserved.

### 1. Introduction

Many advanced optical components present a periodic structuration along two directions of space embedded in a multilayer. An often encountered geometry, for example, consists in a planar waveguide in which holes are drilled periodically. The two-dimensional periodic structuration can be used to monitor the dispersion relation of guided modes [1], to create unpolarized optical filters or sensors [2] or to ameliorate the extraction rate of the emitted light of electroluminescence diode [3]. More recently, it has also been proposed to replace the conventional slide of a microscope by a multilayer cross-grating in order to improve the resolution of the imaging system [4,5].

While many techniques exist to calculate light-scattering by gratings that are invariant along one axis [6,7], there are still very few numerical methods that address the issue of light scattering by crossed gratings. The most commonly used approach is the Fourier modal method [8,9]. This technique which is related to the rigorous coupled wave analysis and to the differential method is efficient for simulating scattering by dielectric 'lamellar' gratings (i.e. motif with vertical walls). Another approach, the C-method, which is based on a change of coordinates, has also been extended to cross-gratings [10]. This approach is particularly efficient for multilayer coated gratings with smoothly varying interfaces. In the microwave domain, a periodic method of moments based on a surface integral was proposed to simulate light scattering by periodic metallic patches embedded in a multilayer. This technique, which is adapted to the design of frequency selective surfaces, is restricted to highly conducting metallic periodic structures as it calculates specifically the surface currents appearing on the patches [11–15].

In this work, we present an alternative numerical approach, based on the coupled dipole method (CDM). Our technique enables to simulate scattering by heterogeneous penetrable doubly periodic structures with arbitrary shape embedded in a multilayer. It is similar to a periodic method of moments [16], but, contrary to the techniques developed in the microwave

\* Corresponding author.

E-mail address: [patrick.chaumet@fresnel.fr](mailto:patrick.chaumet@fresnel.fr) (P.C. Chaumet).

domain for metallic structures, it is based on a volume integral equation and it calculates the local field inside the whole grating cell.

The CDM has been first developed to study light scattering by a tridimensional object with finite dimensions in homogeneous space [17–20]. Then the method has been extended to deal with objects near a substrate (for near-field applications [21] or the study of optical forces [22,23]) and inside a multilayer system [24]. A recent review describes the current state of the CDM and its historical development [25]. Recently, the CDM has been adapted to simulate light scattering by a periodic structure placed above a flat substrate [26]. It has been shown that, when the structure is illuminated by a plane wave, only the base cell of the periodic structure the CDM has to be discretized. In this article, we extend the CDM to periodic structure embedded in a multilayer. We show that this approach can easily deal with double periodic structure where the base cell is made of anisotropic material. This versatile technique should be an interesting complementary tool as compared to those already developed.

## 2. Computation of the field scattered by a periodic structure in a multilayer system

### 2.1. Principle of the CDM

We consider an object placed in a multilayer system. The principle of the CDM consists in modeling the object by a cubic array of  $M$  polarizable subunits [17,16,27]. The electric local field  $\mathbf{E}(\mathbf{r}_i)$  at each subunit position  $\mathbf{r}_i$  can be expressed as

$$\mathbf{E}(\mathbf{r}_i) = \mathbf{E}_0(\mathbf{r}_i) + \sum_{j=1}^M \mathbf{G}(\mathbf{r}_i, \mathbf{r}_j) \alpha(\mathbf{r}_j) \mathbf{E}(\mathbf{r}_j), \quad (1)$$

where  $\mathbf{E}_0(\mathbf{r}_i)$  is the incident field at position  $\mathbf{r}_i$ ,  $\mathbf{G}$  is the field susceptibility tensor of the multilayer system [24].  $\alpha(\mathbf{r}_j)$  is the dynamic polarizability tensor of subunit  $j$ , it includes the radiation reaction term that is required to satisfy the optical theorem [28–30]:

$$\alpha_0(\mathbf{r}_i) = \frac{3d^3}{4\pi} [\varepsilon(\mathbf{r}_i) - \mathbf{I}][\varepsilon(\mathbf{r}_i) + 2\mathbf{I}]^{-1} \quad (2)$$

$$\alpha(\mathbf{r}_i) = \alpha_0(\mathbf{r}_i) [\mathbf{I} - (2/3)ik^3 \alpha_0(\mathbf{r}_i)]^{-1} \quad (3)$$

where  $d$  is the discretization lattice and  $\mathbf{I}$  the unit tensor. The self-consistent field  $\mathbf{E}(\mathbf{r}_i)$  is found by solving the linear system formed by writing Eq. (1) for  $i = 1, \dots, M$ . Notice that the expression  $\mathbf{p}(\mathbf{r}_i) = \alpha(\mathbf{r}_i) \mathbf{E}(\mathbf{r}_i)$  corresponds to the dipole moment of the subunit  $i$  induced by the incident field and the  $M - 1$  other dipoles. Hence  $\mathbf{G}(\mathbf{r}_i, \mathbf{r}_j)$  gives the field radiated at  $\mathbf{r}_i$  by a dipole located at  $\mathbf{r}_j$ . The scattered field at  $\mathbf{r}$  is the sum of the fields radiated by all the dipoles constituting the object [16],

$$\mathbf{E}(\mathbf{r}) = \mathbf{E}_0(\mathbf{r}) + \sum_{j=1}^M \mathbf{G}(\mathbf{r}, \mathbf{r}_j) \alpha(\mathbf{r}_j) \mathbf{E}(\mathbf{r}_j). \quad (4)$$

### 2.2. CDM for periodic structures

The CDM is perfectly adapted to deal with a single object. In the case of a grating, i.e. a periodic duplication of an object over a lattice, see Fig. 1, the number  $M$  of dipoles is infinite and Eq. (1) becomes impossible to solve. Yet, if we assume that the grating is illuminated by a plane wave, it is possible to restrict the linear system, Eq. (1), to the dipoles of one base cell. Indeed, when the incident field is a plane wave with wavevector component parallel to the multilayer plane  $\mathbf{k}_{0\parallel}$ , the field at any position  $\mathbf{r}$  is pseudo-periodic, namely

$$\mathbf{E}(\mathbf{r} + m\mathbf{u} + n\mathbf{v}) = \mathbf{E}(\mathbf{r}) e^{i\mathbf{k}_{0\parallel} \cdot (m\mathbf{u} + n\mathbf{v})}, \quad (5)$$

where  $(m, n) \in \mathbb{Z}^2$  ( $\mathbb{Z}$  denotes the set of all integers).  $\mathbf{u}$  and  $\mathbf{v}$  are the basis vectors of the periodic structure. The self-consistent field at each subunit of the object constituting the base cell of the periodic structure can be written as

$$\mathbf{E}(\mathbf{r}_i) = \mathbf{E}_0(\mathbf{r}_i) + \sum_{j=1}^M \left[ \sum_{m,n=-\infty}^{\infty} \mathbf{G}(\mathbf{r}_i, \mathbf{r}_j + m\mathbf{u} + n\mathbf{v}) e^{i\mathbf{k}_{0\parallel} \cdot (m\mathbf{u} + n\mathbf{v})} \right] \alpha(\mathbf{r}_j) \mathbf{E}(\mathbf{r}_j). \quad (6)$$

Eq. (6) is written for  $i = 1, \dots, M$  and the unknowns are the local field at each subunit constituting the base cell of the grating. Once the local field is found for all  $\mathbf{r}_i$ ,  $i = 1, \dots, M$ , the field scattered at any position  $\mathbf{r}$  is deduced from,

$$\mathbf{E}(\mathbf{r}) = \mathbf{E}_0(\mathbf{r}) + \sum_{j=1}^M \left[ \sum_{m,n=-\infty}^{\infty} \mathbf{G}(\mathbf{r}, \mathbf{r}_j + m\mathbf{u} + n\mathbf{v}) e^{i\mathbf{k}_{0\parallel} \cdot (m\mathbf{u} + n\mathbf{v})} \right] \alpha(\mathbf{r}_j) \mathbf{E}(\mathbf{r}_j). \quad (7)$$

Hence, the main problem of this approach lays in the efficient computation of the periodic field susceptibility in a multilayer system which is given by the infinite sum between the bracket. Once the periodic susceptibility tensor is known

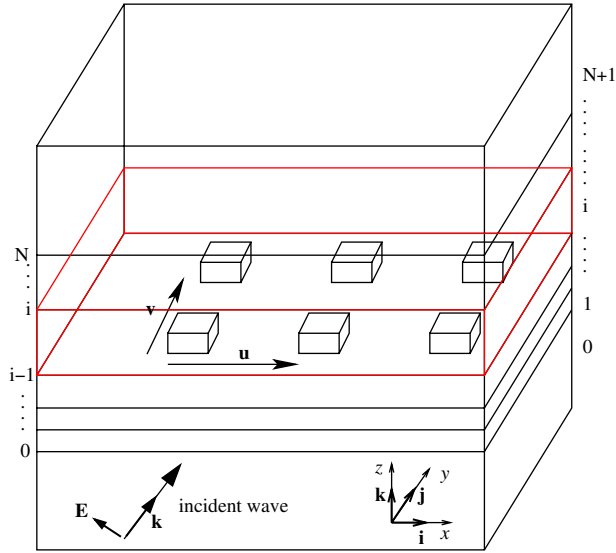


**Fig. 1.** Geometry of the system: a double periodic structure with basis vector  $\mathbf{u}$  and  $\mathbf{v}$  is introduced in a multilayer system. The numbers on the right label the layers while that on the left label the interfaces.

for a given lattice, one can simulate light-scattering by gratings with different motifs but same lattice very rapidly. Thus, this technique appears quite promising for optimization purposes.

### 2.3. Computation of the periodic susceptibility tensor in a multilayer system

The main difficulty of the periodic CDM lies in the computation of the periodic susceptibility tensor which basically gives the field radiated at any observation point by an infinite number of dipoles periodically placed in the multilayer along the grating lattice nodes. Several papers have addressed this problem [31,32].

When the period of the grating is of the order or smaller than the wavelength of illumination it appears more efficient to compute the periodic susceptibility tensor in the Fourier space. Due to the translational invariance of the multilayer system, the periodic susceptibility tensor can be written as,

$$H = \sum_{m,n=-\infty}^{\infty} \mathbf{G}(\mathbf{r}_i, \mathbf{r}_j + m\mathbf{u} + n\mathbf{v}) e^{i\mathbf{k}_{0\parallel} \cdot (m\mathbf{u} + n\mathbf{v})} = \int \sum_{m,n=-\infty}^{\infty} \delta(\mathbf{r}_{\parallel} - m\mathbf{u} - n\mathbf{v}) \mathbf{G}(\boldsymbol{\rho}_{ij} - \mathbf{r}_{\parallel}, z_i, z_j) e^{i\mathbf{k}_{0\parallel} \cdot \mathbf{r}_{\parallel}} d\mathbf{r}_{\parallel} \quad (8)$$

with  $\mathbf{r} = (\mathbf{r}_{\parallel}, z)$  and  $\boldsymbol{\rho}_{ij} = \mathbf{r}_{i\parallel} - \mathbf{r}_{j\parallel}$ . Using the properties of the two-dimensional Fourier transform defined as  $\mathcal{F}[b(\mathbf{r}_{\parallel})] = \int d\mathbf{r}_{\parallel} b(\mathbf{r}_{\parallel}) \exp(-i\mathbf{r}_{\parallel} \cdot \mathbf{h}_{\parallel})$ , and that of its inverse defined as  $\mathcal{F}^{-1}[B(\mathbf{h}_{\parallel})] = 1/(2\pi)^2 \times \int d\mathbf{h}_{\parallel} B(\mathbf{h}_{\parallel}) \exp(i\mathbf{r}_{\parallel} \cdot \mathbf{h}_{\parallel})$ , we get:

$$H = \frac{1}{2\pi^2} \int M \sum_{m,n=-\infty}^{\infty} \delta(\mathbf{k}_{\parallel} - m\mathbf{U} - n\mathbf{V} - \mathbf{k}_{0\parallel}) \mathcal{F}[\mathbf{G}(\boldsymbol{\rho}_{ij} - \mathbf{r}_{\parallel}, z_i, z_j)] d\mathbf{k}_{\parallel} \quad (9)$$

$$= \frac{M}{2\pi^2} \sum_{m,n=-\infty}^{\infty} \mathbb{G}(\boldsymbol{\rho}_{ij}, z_i, z_j, m\mathbf{U} + n\mathbf{V} + \mathbf{k}_{0\parallel}) \quad (10)$$

where  $\mathbf{V} = 2\pi(-u_y\hat{\mathbf{x}} + u_x\hat{\mathbf{y}})/(u_xv_y - v_xu_y)$ ,  $\mathbf{U} = 2\pi(v_y\hat{\mathbf{x}} - v_x\hat{\mathbf{y}})/(u_xv_y - v_xu_y)$  are the basis vectors of the reciprocal lattice, and  $M = (2\pi)^2/(u_xv_y - v_xu_y)$ .  $\hat{\mathbf{x}}$  and  $\hat{\mathbf{y}}$  are the basis vectors of the coordinate system. We will note  $\mathbb{G}(\boldsymbol{\rho}_{ij}, z_i, z_j, \mathbf{k}_{\parallel}) = \mathcal{F}[\mathbf{G}(\boldsymbol{\rho}_{ij} - \mathbf{r}_{\parallel}, z_i, z_j)]$ . The Fourier transform  $\mathbb{G}$  of the periodic susceptibility tensor is easily obtained from the angular spectrum representation of the field diffracted by a dipole in a multilayer system [33],

$$\mathbf{E}_j(\mathbf{r}) = \iint [\mathcal{E}_j^+ e^{i\mathbf{K}_j^+ \cdot \mathbf{r}} + \mathcal{E}_j^- e^{i\mathbf{K}_j^- \cdot \mathbf{r}}] d\mathbf{k}_{\parallel}, \quad (11)$$

$$= \iint \mathbb{G}(\mathbf{r}, \mathbf{r}', \mathbf{k}_{\parallel}) \mathbf{p}(\mathbf{r}') d\mathbf{k}_{\parallel} \quad (12)$$

where  $j$  ( $j = 0, \dots, N + 1$ ) denotes the layer where the observation point is located. The field in each layer is considered as an infinite sum of up and down propagating plane waves. The superscript  $+$  indicates the plane waves propagating towards the positive  $z$ -axis while the superscript  $-$  denotes the plane wave propagating towards the negative  $z$ -axis. The wave vector of these plane waves are  $\mathbf{K}_j^+ = (k_x, k_y, w_j)$  and  $\mathbf{K}_j^- = (k_x, k_y, -w_j)$  with  $k_j^2 = \mathbf{K}_j^+ \cdot \mathbf{K}_j^+ = \mathbf{K}_j^- \cdot \mathbf{K}_j^- = k_{\parallel}^2 + w_j^2 = \epsilon_j k_0^2$ . Moreover we have  $\mathbf{K}_j^+ \cdot \mathcal{E}_j^+ = 0$  and  $\mathbf{K}_j^- \cdot \mathcal{E}_j^- = 0$ . The complex magnitudes of  $\mathcal{E}_j^{\pm}$  are obtained by accounting for the boundary conditions at each interface [33,34,24].

## 2.4. Computational remarks

Once  $\mathbb{G}$  is known, the main numerical difficulty lays in the convergence of the sum appearing in Eq. (10). When the dipole and the observation point do not have the same altitude, the term  $e^{i w_j |z-z'|}$  decays exponentially when  $(m, n)$  are increased. In this case, the convergence is rapidly obtained. On the contrary, when the observation point and the dipole have the same altitude, i.e.  $z = z'$ , the convergence may be very slow. We recall that  $H$  gives the field diffracted at  $\mathbf{r}_i$  by a periodic array of dipoles located at  $\mathbf{r}_j + m\mathbf{u} + n\mathbf{v}$ . When the dipole and observation point are in the same layer, one can distinguish two contributions for the diffracted field, one corresponding to the direct propagation between the set of dipoles and the observation point (as if the dipoles were in a homogeneous space), and the second corresponding to the propagation between the set dipoles and the observation point through the multiple reflections in the multilayer. Only the first contribution, i.e. the direct term, is responsible for the slow convergence of the series. Hence, to accelerate the convergence we compute separately this first contribution. When the layer containing the dipole and observation point has a complex relative permittivity (namely the layer is absorbing) the sum is performed in the direct space. If the relative permittivity of the layer is real, one splits the infinite sum terms in two parts; one in the direct space and one in the reciprocal space, where these two sums converge quickly owing to a damping function [35].

## 3. Numerical examples

### 3.1. Comparisons between the periodic CDM and the Fourier modal method

In our first example, we compare the field transmitted by an isotropic layered grating calculated by the periodic CDM with that given by the Fourier modal method [8]. The system under study consists in a square array of pads with relative permittivity  $\epsilon_p$  embedded in a dielectric layer of relative permittivity  $\epsilon_l$  and deposited on a glass substrate, see Figs. 2(a) and (b). The illumination is a TM polarized plane wave coming from the substrate in the  $(x, z)$  plane. Notice that all the chosen examples involve only one layer. However, the method can easily deal with multilayer systems.

In Figs. 2(c) and (d) we plot the intensity of the field at  $z = \lambda/30$ ,  $x = 0$  for the CDM and the Fourier modal method for two angles of incidence and two different permittivity contrast between the pads and the layer. Fig. 2(c) shows a very good

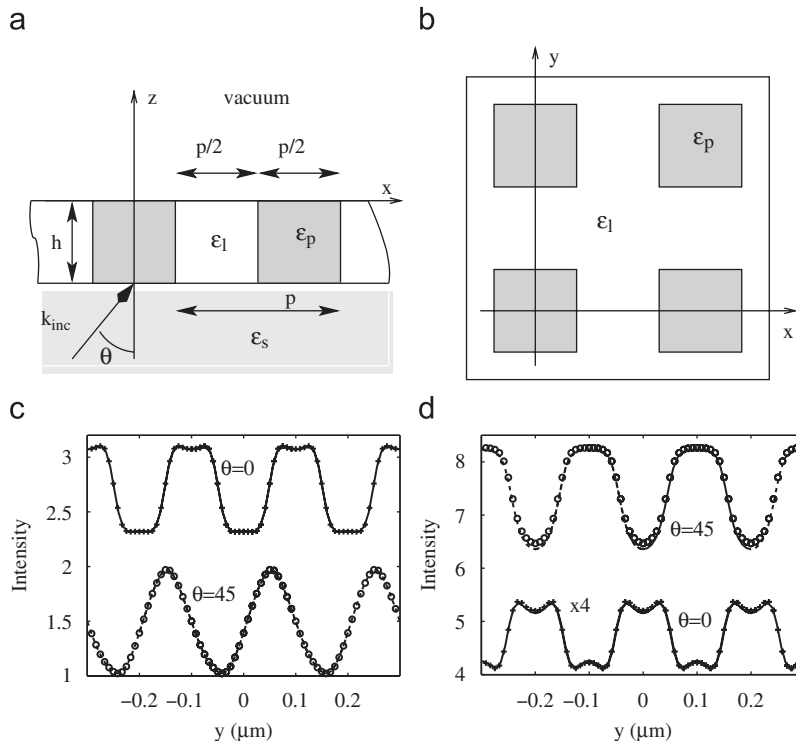


**Fig. 2.** Geometry of the cross-grating. The grating is illuminated from the substrate. The grating is made of a square array of cubic pads of relative permittivity ( $\epsilon_p$ ) embedded in a layer of relative permittivity  $\epsilon_l$  deposited on a substrate with relative permittivity  $\epsilon_s$ . The height of the layer is equal to the width of the pads  $p = h = \lambda/3$ . The period of the grating with square lattice is twice the width of the pads. (a) Side view. (b) Top view. (c) and (d) plot of the intensity of the electric field at  $z = \lambda/30$  for  $x = 0$ . (plain line) CDM and (crosses) Fourier modal method simulations for  $\theta = 0^\circ$ . (dashed line) CDM and (circles) Fourier modal method simulations for  $\theta = 45^\circ$ . (c)  $\epsilon_s = \epsilon_p = 2.25$  and  $\epsilon_l = 1$ . (d)  $\epsilon_s = \epsilon_p = 9$  and  $\epsilon_l = 4$ .

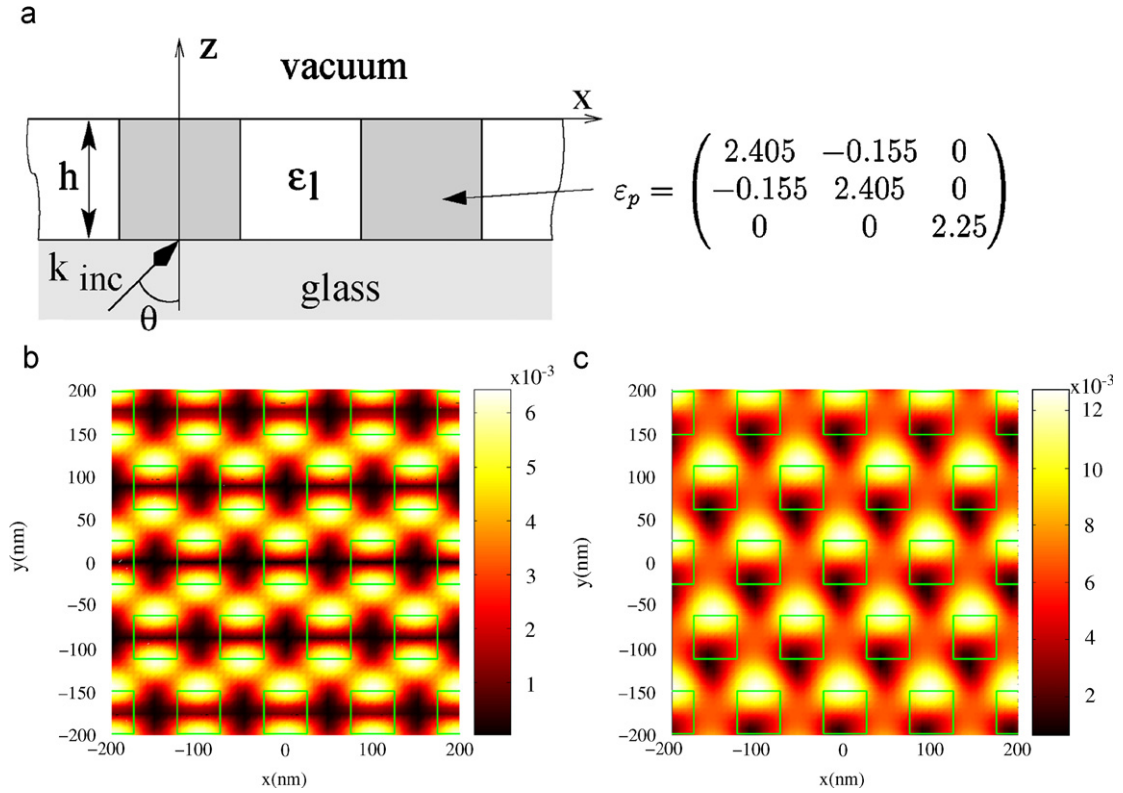


**Fig. 3.** (a) The grating consists in an hexagonal array of cubic pads with  $\mathbf{u} = (\lambda/6, 0)$  and  $\mathbf{v} = (\sqrt{3}\lambda/12, \lambda/12)$  and  $h = \lambda/6$ . The pads are indicated with green squares in (b) and (c). A TM polarized incident plane wave illuminates the grating under internal reflexion with  $\theta = 45^\circ$ . (b) The pads are made of glass  $\epsilon_p = 2.25$  and are embedded in a layer with  $\epsilon_l = 4$ . The substrate is glass with  $\epsilon = 2.25$ . The component  $y$  of the field is represented in the plane  $(x, y)$  at  $z = \lambda/12$ . (c) Same as (b) but the pads are made of anisotropic material (see the text).

agreement between the CDM and the Fourier modal method. The relative difference between both methods is always less than 2%.

### 3.2. Anisotropic grating

To point out the versatility of our method, we also show the field transmitted by an hexagonal array of anisotropic pads embedded in an isotropic dielectric layer. The geometry is shown in Fig. 3(a). The pads are uniaxial with a difference between the extraordinary and ordinary index  $\Delta = n_o - n_e = 0.1$ . The axis of the relative permittivity tensor are not confounded with the axis of the system, so that the relative permittivity tensor is non diagonal (the eigenvectors are  $(\sqrt{2}, \sqrt{2}, 0)$ ,  $(\sqrt{2}, -\sqrt{2}, 0)$  and  $(0, 0, 1)$ ). The illumination is a TM polarized plane wave in the plane  $(x, z)$  with  $\theta = 45^\circ$  coming from the substrate, hence without the grating we get an evanescent wave above the layer: the critical angle is  $\theta_c = 41.8^\circ$ . The effect of the anisotropy is particularly strong for the  $y$  component of the field, see Fig. 3(b) for isotropic pads and Fig. 3(c) for anisotropic pads. As expected, the  $x$ -symmetry is lost in the case of anisotropic pads.

## 4. Conclusion

In this work we have extended the Coupled Dipole Method to simulate light scattering by doubly periodic structures placed in a multilayer system. There are still very few methods that are able to perform this kind of simulations. The advantage of our approach is its versatility. In particular, accounting for heterogeneous structures made of anisotropic material does not add any computational difficulty. The main difficulty of this technique lies in the computation of the periodic susceptibility tensor that gives the field radiated by an array of dipoles placed in a multilayer system. Once it is known, the simulation of the field scattered by gratings with different motifs but same lattice requires small computation time. Hence, this approach seems to be an adequate tool for optimization purposes. The mixed representation of the field in both the direct and Fourier space renders this technique complementary to the classical Fourier modal method where the field is calculated exclusively in the Fourier Space.

## References

- [1] Johnson SG, Fan SH, Villeneuve PR, Joannopoulos JD, Kolodziejski LA. Guided modes in photonic crystal slabs. *Phys Rev B* 1999;60:5751–8.
- [2] Fehrembach AL, Talneau A, Boyko O, Lemarchand F, Sentenac A. Experimental demonstration of a narrowband, angular tolerant, polarization independent, doubly periodic resonant grating filter. *Opt Lett* 2007;32:2269–71.
- [3] Fehrembach AL, Enoch S, Sentenac A. Highly directive source devices using slab photonic crystal. *Appl Phys Lett* 2001;79:4280–2.
- [4] Chaumet PC, Sentenac A. Numerical simulations of the electromagnetic field scattered by defects in a double-periodic structure. *Phys Rev B* 2005;72:205437–8.
- [5] Sentenac A, Chaumet PC, Belkebir K. Beyond the Rayleigh criterion: grating assisted far-field optical diffraction tomography. *Phys Rev Lett* 2006;97:243901.
- [6] Petit R. *Electromagnetic theory of gratings*. Berlin: Springer; 1980.
- [7] Demesy G, Zolla F, Nicolet A, Commandre MFC. The finite element method as applied to the diffraction by an anisotropic grating. *Opt Express* 2007;15:18089–102.
- [8] Li L. New formulation of the Fourier modal method for crossed surface-relief gratings. *J Opt Soc Am A* 1997;14:2758–67.
- [9] Li L. Fourier modal method for crossed anisotropic gratings with arbitrary permittivity and permeability tensors. *J Opt A* 2003;5:345–55.
- [10] Granet G. Analysis of diffraction by surface-relief crossed gratings with use of the Chandezon method: application to multilayer crossed gratings. *J Opt Soc Am A* 1998;15:1121–31.
- [11] Blackburn J, Arnaut LR. Numerical convergence in periodic method of moments analysis of frequency-selective surfaces based on wire elements. *IEEE Trans Antennas Propagat* 2005;53(10):3308–15.
- [12] Bozzi M, Perregini L. Analysis of multilayered printed frequency selective surfaces by the MoM/BI-RME method. *IEEE Trans Antennas Propagat* 2003;51:2830–6.
- [13] Luebbers RJ, Munk BA. Some effects of dielectric loading on periodic slot arrays. *IEEE Trans Antennas Propagat* 1978;26:536–42.
- [14] Monacelli B, Boreman G, Pryor J, Munk BA, Kotter D. Infrared frequency selective surfaces. *IEEE Trans Antennas Propagat. Society International Symposium 2004*;2:2175–8.
- [15] Schneider SW, Munk BA. The scattering properties of super dense arrays of dipoles. *IEEE Transactions on Antennas and Propagation* 1994;42:463–72.
- [16] Chaumet PC, Sentenac A, Rahmani A. Coupled dipole method for scatterers with large permittivity. *Phys Rev E* 2004;70:036606–6.
- [17] Purcell EM, Pennypacker CR. Scattering and absorption of light by nonspherical dielectric grains. *Astrophys J* 1973;186:705–14.
- [18] Draine BT, Flatau PJ. Discrete-dipole approximation for scattering calculations. *J Opt Soc Am A* 1994;11:1491–9.
- [19] Flatau PJ, Stephens GL, Draine BT. Light scattering by rectangular solids in the discrete-dipole approximation: a new algorithm exploiting the Block-Toeplitz structure. *J Opt Soc Am A* 1990;7:593–600.
- [20] Yurkin MA, Maltsev VP, Hoekstra AG. The discrete dipole approximation for simulation of light scattering by particles much larger than the wavelength. *JQSRT* 2007;106:546–57.
- [21] Chaumet PC, Rahmani A, de Fornel F, Dufour J-P. Evanescent light scattering: the validity of the dipole approximation. *Phys Rev B* 1998;58:2310–5.
- [22] Chaumet PC, Rahmani A, Nieto-Vesperinas M. Selective nanomanipulation using optical forces. *Phys Rev B* 2002;66:195405–11.
- [23] Chaumet PC, Rahmani A, Nieto-Vesperinas M. Photonic force spectroscopy on metallic and absorbing nanoparticles. *Phys Rev B* 2005;71:045425–7.
- [24] Paulus M, Gay-Balmaz P, Martin OJF. Accurate and efficient computation of the Green's tensor for stratified media. *Phys Rev E* 2000;62(4):5797–807.
- [25] Yurkin MA, Hoekstra AG. The discrete dipole approximation: an overview and recent developments. *JQSRT* 2007;106:558–89.
- [26] Chaumet PC, Rahmani A, Bryant GW. Generalization of the coupled dipole method to periodic structure. *Phys Rev B* 2003;67:165404–5.
- [27] Rahmani A, Chaumet PC, Bryant GW. On the importance of local-field corrections for polarizable particles on a finite lattice: application to the discrete dipole approximation. *Astrophys J* 2004;607:873–8.
- [28] Lakhtakia A. Strong and weak forms of the method of moments and the coupled dipole method for scattering of time-harmonic electromagnetics fields. *Int J Mod Phys C* 1992;3:583–603.
- [29] Chaumet PC. Comment on “Trapping force, force constant, and potential depths for dielectric spheres in the presence of spherical aberrations”. *Appl Opt* 2004;43:1825–6.
- [30] Rahmani A, Chaumet PC, Bryant GW. Local-field correction for an interstitial impurity in a crystal. *Opt Lett* 2002;27:430–2.
- [31] Shubair RM. Fast and accurate method-of-moment solution of vertical antennas in contiguous dielectric half-spaces using closed-form spatial Green's functions. *IEEE Trans Antennas Propagat. Society International Symposium 1999*;4:827–30.
- [32] Wang D, Yung EKN, Chen RS, Ding DZ, Tang WC. On evaluation of the Green function for periodic structures in layered media. *IEEE Antennas and Wireless Propagation Letters* 2004;3:133–6.
- [33] Agarwal GS. Quantum electrodynamics in the presence of dielectrics and conductors. I. Electromagnetic-field response functions and black-body fluctuations in finite geometry. *Phys Rev A* 1975;11:230–42.
- [34] Sipe JE. New green-function formalism for surface optics. *J Opt Soc Am B* 1987;4:481–9.
- [35] Poppe GPM, Wijers CMJ, van Silfhout A. IR spectroscopy of CO physisorbed on NaCl(100): Microscopic treatment. *Phys Rev B* 1991;44:7917–29.